PAPER Special Section on Advanced RF Technologies for Compact Wireless Equipment and Mobile Phones

Synthesizing Microstrip Dual-Band Bandpass Filters Using Frequency Transformation and Circuit Conversion Technique

Xuehui GUAN[†], *Nonmember*, **Zhewang MA**[††a)], *Member*, **Peng CAI**[†], *Nonmember*, **Yoshio KOBAYASHI**[††], *Fellow*, **Tetsuo ANADA**[†††], *Member*, *and* **Gen HAGIWARA**[††††], *Nonmember*

SUMMARY A novel method is proposed to synthesize dual-band bandpass filters (BPFs) from a prototype lowpass filter. By implementing successive frequency transformations and circuit conversions, a new filter topology is obtained which consists of only admittance inverters and series or shunt resonators, and is thereby easy to be realized by using conventional distributed elements. A microstrip dual-band BPF with central frequencies of 1.8 GHz and 2.4 GHz is designed and fabricated using microstrip lines and stubs. The simulated and measured results show a good agreement and validate thereby the proposed theory.

key words: *admittance inverter, dual-band filter, frequency transformation, microstrip line*

1. Introduction

Rapid developments of modern communications demand efficient utilization of more and more frequency channels. To reduce the volume and weight of communication circuits and equipments, many dual-band and multi-band components, including antennas [1], amplifiers [2], and microwave filters [3]–[6] have been developed. A number of publications have provided a variety of solutions to the realization of dual-band bandpass filters (BPFs). Miyake et al. [3] used parallel-connected two different filters to obtain dual-band characteristics. Tsai and Hsue [4] inserted a stopband into a broadband to form dual-bands by cascading a broadband filter with a bandstop filter. Because the circuit configurations in both [3] and [4] include two different filters, the sizes of these dual-band filters are comparatively large. Recently, Chang et al. reported dual-band BPFs employing stepped impedance resonators (SIRs) [5], [6]. One of the advantages of the SIR filter is that the positions of the dual-bands can be designed conveniently. However, it confronts difficulties when making adjustment of coupling coefficients between neighboring resonators to meet simultaneously the dual bandwidth specifications of the filter.

Uchida et al. [7] developed a dual-band-rejection filter with smaller passband insertion loss through the formation of two closely spaced rejection bands, using a novel frequency-transformation. This frequency-transformation technique was extended to the synthesis of dual-band BPFs in [8]. In this paper, the synthesis theory is expanded with detailed description of the formulas and circuits, filtering characteristics, realization problems of the dual-band filter using distributed transmission lines, and discussions on the advantages and disadvantages of the method compared with previous related approaches.

The theory commences with a conventional prototype lowpass filter (LPF) and a frequency transformation, which converts the prototype LPF into a BPF. After a second frequency transformation is carried out, the BPF is converted into a dual-band BPF. The dual-band BPF owns a complicated configuration compared with those of conventional BPFs. To simplify the realization of the obtained dual-band BPF using distributed transmission lines or waveguides, admittance inverters are introduced successively to evolve the filter into new topologies. The final circuitry of the dual-band filter consists of only series or shunt *LC* resonators and admittance inverters, and hence can be easily realized by using distributed transmission lines and conventional design techniques. To verify the proposed theory, a dual-band BPFs operating at 1.8 GHz and 2.4 GHz is designed and fabricated in a microstrip form. It is found that the measured response of the filter agrees well with the simulated result.

2. Theory

2.1 Two-Pole Dual-Band BPF

Figure 1 shows a two-pole prototype LPF and its transmission characteristics. The element values of g_0, g_1, g_2, and g_3 in the prototype filter are determined by its passband specifications using the well-known formulas in [9], and ε is a constant relating to the maximum insertion loss in the passband.

The prototype LPF is converted to a bandpass filter by

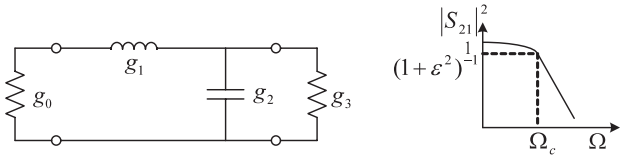

Fig. 1 The prototype lowpass filter and its transmission characteristics.

Manuscript received August 31, 2005.
Manuscript revised November 25, 2005.

[†]The authors are with the School of Communication and Information Engineering, Shanghai University, Shanghai 200072, China.
[††]The authors are with the Department of Electrical and Electronic Systems, Saitama University, Saitama-shi, 338-8570 Japan.
[†††]The author is with the High-Tech Research Center, Kanagawa University, Yokohama-shi, 221-8686 Japan.
[††††]The author is with the Link Circuit Inc., Saitama-shi, 336-0917 Japan.
a) E-mail: ma@ees.saitama-u.ac.jp
DOI: 10.1093/ietele/e89–c.4.495

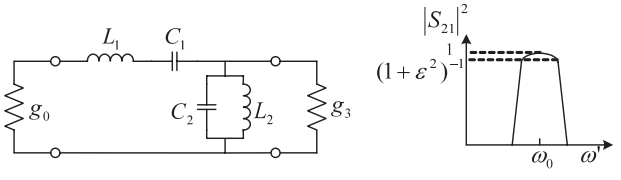

Fig. 2 Two-pole bandpass filter and its transmission characteristics.

executing the following frequency transformation [9]:

$$\Omega \rightarrow \frac{\Omega_c}{FBW_0}\left(\frac{\omega'}{\omega_0} - \frac{\omega_0}{\omega'}\right) \tag{1}$$

where Ω and ω' are angular frequencies of the LPF and BPF, respectively, Ω_c=1 radian/s is the cutoff angular frequency of the prototype LPF, FBW_0 and ω_0 are the fractional bandwidth and center frequency of the BPF, respectively. Through this transformation, the series inductor and shunt capacitor in the LPF are converted to a series and a shunt LC resonator, respectively, in the bandpass filter shown in Fig. 2. The schematic transmission response of the BPF is also given in Fig. 2. The expressions for the circuit elements in Fig. 2 are as follows:

$$L_1 = \frac{g_1\Omega_c}{FBW_0\omega_0}, \quad C_1 = \frac{1}{L_1\omega_0^2} \tag{2}$$

$$L_2 = \frac{FBW_0}{g_2\Omega_c\omega_0}, \quad C_2 = \frac{1}{L_2\omega_0^2} \tag{3}$$

The bandpass filter is further converted to a dual-band BPF when the following frequency transformation [7] is conducted:

$$\omega' = \frac{\omega_0}{\omega_2 - \omega_1}\left(\omega - \frac{\omega_1\omega_2}{\omega}\right) = \frac{\omega_0}{FBW}\left(\frac{\omega}{\omega_0} - \frac{\omega_0}{\omega}\right) \tag{4}$$

where ω is the angular frequency of the dual-band BPF, ω_1 and ω_2 are the center angular frequencies of the first and second passband of the dual-band filter, FBW= $(\omega_2 - \omega_1)/\omega_0$, and $\omega_0 = (\omega_1\omega_2)^{1/2}$.

In the case of a narrow band (e.g., $FBW_1 < 0.1$) filter, our derivation reveals

$$FBW_1 = FBW_2 = FBW_0\frac{\omega_2 - \omega_1}{\omega_1 + \omega_2} \tag{5}$$

here FBW_1 and FBW_2 are the fractional bandwidths of the first and second passband of the dual-band filter, respectively. Through this transformation, the inductor and capacitor in the BPF are converted to a series and a shunt LC resonator, respectively. The circuit configuration of the obtained two-pole dual-band BPF is shown in Fig. 3, where the schematic transmission characteristics of the filter are also depicted. Through a little bit tedious but straightforward formulation, we get expressions for the circuit elements in Fig. 3 as follows:

$$L_{11} = \frac{g_1\Omega_c}{FBW_0(\omega_2 - \omega_1)}, \quad C_{11} = \frac{1}{L_{11}\omega_0^2} \tag{6}$$

$$L_{12} = \frac{g_1\Omega_c(\omega_2 - \omega_1)}{FBW\omega_0^2}, \quad C_{12} = \frac{1}{L_{12}\omega_0^2} \tag{7}$$

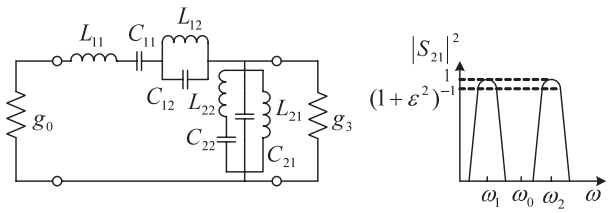

Fig. 3 Two-pole dual-band BPF and its transmission characteristics.

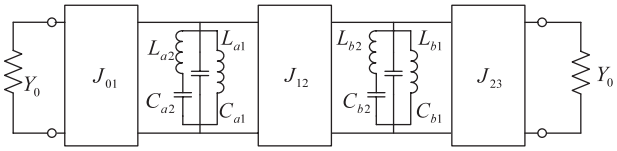

Fig. 4 Dual-band BPF with J-inverters, series and shunt LC resonators.

$$L_{21} = \frac{FBW(\omega_2 - \omega_1)}{g_2\Omega_c\omega_0^2}, \quad C_{21} = \frac{1}{L_{21}\omega_0^2} \tag{8}$$

$$L_{22} = \frac{FBW}{g_2\Omega_c(\omega_2 - \omega_1)}, \quad C_{22} = \frac{1}{L_{22}\omega_0^2} \tag{9}$$

It is observed that the circuit configuration of the dual-band BPF in Fig. 3 becomes fairly complicated compared with that of the conventional BPF in Fig. 2. Its series and shunt branches now include both series and shunt LC resonators. Such a circuit is difficult to realize at microwave frequencies when using distributed transmission lines. Therefore, successive circuit conversions are implemented below. First, the series branch is replaced by a shunt branch with the aid of admittance inverters (J-inverters), as is shown in Fig. 4. Circuit elements in Fig. 4 are determined by the following expressions:

$$L_{ai} = \frac{g_0Y_0}{J_{01}^2}C_{1i}, \; L_{bi} = \frac{J_{01}^2}{g_0Y_0J_{12}^2}L_{2i}, \; i = 1, 2 \tag{10}$$

$$L_{a1}C_{a1} = L_{a2}C_{a2} = L_{b1}C_{b1} = L_{b2}C_{b2} = \frac{1}{\omega_0^2} \tag{11}$$

$$J_{12} = \frac{J_{01}J_{23}}{Y_0}\sqrt{\frac{g_3}{g_0}} \tag{12}$$

Although the circuit in Fig. 4 contains only shunt branches now, each of the shunt branches includes both series and shunt LC resonators. Therefore, a further step of circuit conversion is implemented by replacing all the shunt resonators with series resonators through the assistance of admittance inverters. The obtained filter is shown in Fig. 5, which consists of J-inverters and series LC resonators only. The derived formulas for the circuit elements in Fig. 5 are given below:

$$J_a = J_{01}\sqrt{\frac{C_{x1}}{g_0Y_0C_{11}}}, \; J_b = J_{23}\sqrt{\frac{g_3C_{x2}}{Y_0L_{21}}} \tag{13}$$

$$L_{x1}C_{x1} = L_{x2}C_{x2} = \frac{1}{\omega_0^2} \tag{14}$$

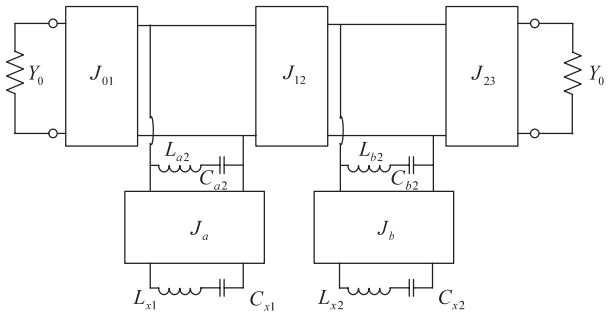

Fig. 5 Dual-band BPF with J-inverters and series LC resonators only.

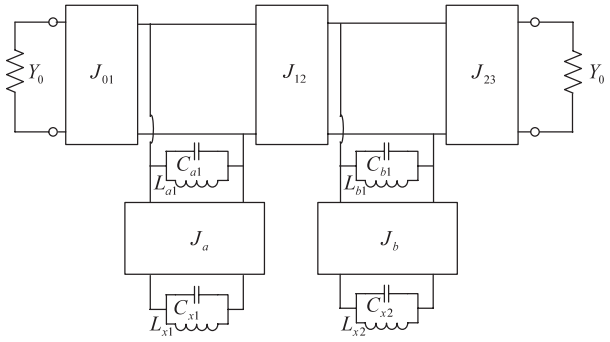

Fig. 6 Dual-band BPF with J-inverters and shunt LC resonators only.

Another possible choice of circuit conversion is shown in Fig. 6, which is obtained by replacing all the series resonators in Fig. 4 with shunt LC resonators through the use of admittance inverters. The circuit elements in Fig. 6 are expressed by:

$$J_a = J_{01}\sqrt{\frac{C_{x1}}{g_0 Y_0 C_{12}}},\ J_b = J_{23}\sqrt{\frac{g_3 C_{x2}}{Y_0 L_{22}}} \tag{15}$$

$$L_{x1}C_{x1} = L_{x2}C_{x2} = \frac{1}{\omega_0^2} \tag{16}$$

Now the dual-band filters in Figs. 5 and 6 contain only a single type of resonator, either series or shunt resonator, so they can be easily implemented by using distributed transmission lines or waveguides. Theoretically the elements C_{x1}, C_{x2}, J_{01} and J_{23} in (13) and (14), or in (15) and (16), may take arbitrary values. However, in practice, their values need to be chosen appropriately so that physical dimensions of these elements can be realized without much difficulty. The admittance inverters, J_{12}, J_a, and J_b, and in Figs. 5 and 6 are then determined by using (13) or (15), respectively. The flexibility in the choice of the parameters allows us more freedom in the design and realization of dual-band BPFs.

2.2 N-Pole Dual-Band BPF

The theory described above is extended to an n-pole dual-band filter by following the same frequency transformation and circuit conversion process. After the first and second frequency transformation, the circuit of an n-pole dual-band

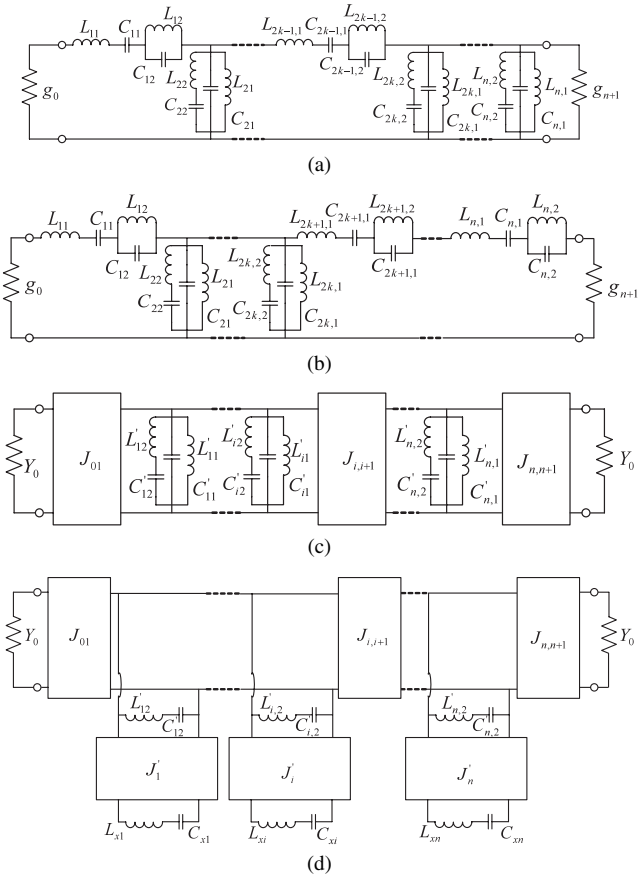

Fig. 7 (a) Circuit of an n-pole dual-band BPF when n is even. (b) Circuit of an n-pole dual-band BPF when n is odd. (c) n-pole dual-band BPF with J-inverters, series and shunt LC resonators. (d) n-pole dual-band BPF with J-inverters and series LC resonators only.

BPF is shown in Fig. 7(a) in the case of an even number of n, and shown in Fig. 7(b) in the case of an odd number of n. Expressions for the circuit elements in Fig. 7(a) are as follows:

$$L_{2k-1,1} = \frac{g_{2k-1}\Omega_c}{FBW_0(\omega_2-\omega_1)},\ C_{2k-1,1} = \frac{1}{L_{2k-1,1}\omega_0^2} \tag{17}$$

$$L_{2k-1,2} = \frac{g_{2k-1}\Omega_c(\omega_2-\omega_1)}{FBW_0\omega_0^2},\ C_{2k-1,2} = \frac{1}{L_{2k-1,2}\omega_0^2} \tag{18}$$

$$L_{2k,1} = \frac{FBW_0(\omega_2-\omega_1)}{g_{2k}\Omega_c\omega_0^2},\quad C_{2k,1} = \frac{1}{L_{2k,1}\omega_0^2} \tag{19}$$

$$L_{2k,2} = \frac{FBW_0}{g_{2k}\Omega_c(\omega_2-\omega_1)},\quad C_{2k,2} = \frac{1}{L_{2k,2}\omega_0^2} \tag{20}$$

where n is even, and $k = 1, 2, \ldots, n/2$. Expressions for the circuit elements in Fig. 7(b) are given by

$$L_{2k,1} = \frac{FBW_0(\omega_2-\omega_1)}{g_{2k}\Omega_c\omega_0^2},\quad C_{2k,1} = \frac{1}{L_{2k,1}\omega_0^2} \tag{21}$$

$$L_{2k,2} = \frac{FBW_0}{g_{2k}\Omega_c(\omega_2-\omega_1)},\quad C_{2k,2} = \frac{1}{L_{2k,2}\omega_0^2} \tag{22}$$

$$L_{2k+1,1} = \frac{g_{2k+1}\Omega_c}{FBW_0(\omega_2-\omega_1)},\ C_{2k+1,1} = \frac{1}{L_{2k+1,1}\omega_0^2} \tag{23}$$

$$L_{2k+1,2}=\frac{g_{2k+1}\Omega_c(\omega_2-\omega_1)}{FBW_0\omega_0^2},\ C_{2k+1,2}=\frac{1}{L_{2k+1,2}\omega_0^2} \tag{24}$$

where n is odd, and $k = 0, 1, 2, \ldots, (n-1)/2$.

By implementing the first and second circuit conversion using J-inverters, as described above for the 2-pole filter, the n-pole dual-band BPF in Fig. 7(a) or 7(b) is transformed first to a configuration shown by Fig. 7(c), and then to the one shown by Fig. 7(d) which includes only series LC resonators and J-inverters. Circuit elements in Figs. 7(c) and 7(d) are determined by the following expressions:

$$L'_{2k-1,1}=\frac{g_0Y_0J_{12}^2\cdots J_{2k-3,2k-2}^2}{J_{01}^2\cdots J_{2k-2,2k-1}^2}C_{2k-1,1},\ C'_{2k-1,1}=\frac{1}{L'_{2k-1,1}\omega_0^2} \tag{25}$$

$$L'_{2k-1,2}=\frac{g_0Y_0J_{12}^2\cdots J_{2k-3,2k-2}^2}{J_{01}^2\cdots J_{2k-2,2k-1}^2}C_{2k-1,2},\ C'_{2k-1,2}=\frac{1}{L'_{2k-1,2}\omega_0^2} \tag{26}$$

$$L'_{2k,1}=\frac{J_{01}^2\cdots J_{2k-2,2k-1}^2}{g_0Y_0J_{12}^2\cdots J_{2k-1,2k}^2}L_{2k,1},\ C'_{2k,1}=\frac{1}{L'_{2k,1}\omega_0^2} \tag{27}$$

$$L'_{2k,2}=\frac{J_{01}^2\cdots J_{2k-2,2k-1}^2}{g_0Y_0J_{12}^2\cdots J_{2k-1,2k}^2}L_{2k,2},\ C'_{2k,2}=\frac{1}{L'_{2k,2}\omega_0^2} \tag{28}$$

$$J_{n,n+1}=\frac{Y_0J_{12}\cdots J_{2k-1,2k}\cdots J_{n-1,n}}{J_{01}\cdots J_{2k,2k+1}\cdots J_{n-2,n-1}}\sqrt{\frac{g_0}{g_{n+1}}} \tag{29}$$

in the case when n is even, and $k = 1, 2, \ldots, n/2$, or by expressions given below:

$$L'_{2k,1}=\frac{J_{01}^2\cdots J_{2k-2,2k-1}^2}{g_0Y_0J_{12}^2\cdots J_{2k-1,2k}^2}L_{2k,1},\ C'_{2k,1}=\frac{1}{L'_{2k,1}\omega_0^2} \tag{30}$$

$$L'_{2k,2}=\frac{J_{01}^2\cdots J_{2k-2,2k-1}^2}{g_0Y_0J_{12}^2\cdots J_{2k-1,2k}^2}L_{2k,2},\ C'_{2k,2}=\frac{1}{L'_{2k,2}\omega_0^2} \tag{31}$$

$$L'_{2k+1,1}=\frac{g_0Y_0J_{12}^2\cdots J_{2k-1,2k}^2}{J_{01}^2\cdots J_{2k,2k+1}^2}C_{2k+1,1},\ C'_{2k+1,1}=\frac{1}{L'_{2k+1,1}\omega_0^2} \tag{32}$$

$$L'_{2k+1,2}=\frac{g_0Y_0J_{12}^2\cdots J_{2k-1,2k}^2}{J_{01}^2\cdots J_{2k,2k+1}^2}C_{2k+1,2},\ C'_{2k+1,2}=\frac{1}{L'_{2k+1,2}\omega_0^2} \tag{33}$$

$$J_{n,n+1}=\frac{J_{01}\cdots J_{2k,2k+1}\cdots J_{n-1,n}}{J_{12}\cdots J_{2k-1,2k}\cdots J_{n-2,n-1}}\sqrt{\frac{g_{n+1}}{g_0}} \tag{34}$$

in the case when n is odd, and k=0, 1,2, …,(n−1)/2. Other additional formulas for the circuit elements in Fig. 7(d) are:

$$J'_i=\sqrt{\frac{C_{xi}}{L'_{i1}}},\quad i=1,2,\cdots n \tag{35}$$

$$C_{xi}L_{xi}=\frac{1}{\omega_0^2},\quad i=1,2,\cdots n \tag{36}$$

2.3 Discussions

The above formulation process shows that the proposed method owns the following distinctive features: (1) First, it starts form the conventional prototype lowpass filter which is familiar to most filter designers. The frequency transformation and circuit conversion are straightforward, and the obtained closed-form design formulas are simple and easy to use. (2) Second, the derived design formulas provide direct relations between the specifications of a dual-band filter and the circuit element values. Therefore, from given specifications of a dual-band filter, all the circuit parameters can be determined readily by using these formulas. (3) Third, the final circuit consists of only series or shunt resonators and J-inverters, so it can be easily realized by using distributed transmission line structures and traditional design techniques and experiences.

In [10] and [11], dual-band filters consisting of microstrip lines and short- or open-circuited stubs are also investigated. In [10], Wada et al. suggested the use of capacitor-loaded open stubs for possible applications to dual-passband filters. Innovative discussions on the introduction of transmission zeros between two passbands in order to increase the in-between isolations were made. But only schematic transmission line models of the filter were given, and no design formulas were provided to relate the filter specifications and circuit parameters. In [11], also only schematic transmission line model consisting of cascaded short-circuited or/and open- circuited stubs and lines was considered. The electrical lengths and characteristics impedances of the lines and stubs were chosen as optimization variables, and by using annealing algorithm, optimum design of the filter was performed to get the physical dimensions of the filter. As stated by the authors of [11], no equivalent circuit model was needed. However, it is evident that the computation cost of the annealing algorithm is significantly higher than that of the closed-form design formulas of this paper. Moreover, this annealing algorithm cannot assure that an optimum solution can always be obtained. In some cases, the solution may contain redundant stubs in the filter configuration which in turn results in a larger circuit space occupation.

The present method has also some shortcomings. First, it is basically appropriate for the design of narrow band (e.g., less than 10%) filters. But this limitation is not a problem in many cases of filter applications. Second, although the central frequencies of the dual passbands can be chosen separately, the formulation process above requires that the fractional bandwidths of the first and second passbands are equal. This requirement may introduce a limit to the wide acceptance of the proposed method. But in the practical design of the filter, we find that the dual passbands can be controlled separately to some extent through the adjustment of the circuit parameters. Third, the J-inverters in the circuit are required unvaried at the center frequencies of two passbands. This is usually not true when the inverters are realized by distributed structures. This problem is also encountered by most previous design methods of dual-band filters. Some recent papers invented the designed of dual-band inverters [12], [13]. A more simple method is just to

use quarter-wavelength transmission lines [14] at the average frequency $\omega_0 = (\omega_1\omega_2)^{1/2}$ of the dual-bands. This simple implementation of the J-inverters will cause the mid-band frequencies of the dual-bands moving a little bit closer. Since the focus of this paper is on the new synthesis method and design formulas, the simplified model of a J-inverter using quarter-wavelength transmission line is used in the following design example.

3. Design and Realization

In order to validate the theory proposed above, we try to design a dual-band filter based on the circuit topology shown in Fig. 5 or 6, and realize it using microstrip lines. As mentioned above, it is straightforward to realize the admittance inverters in Fig. 5 or 6 by employing microstrip quarter-wavelength lines. On the other hands, the series LC resonators can be realized by using microstrip quarter-wavelength open stubs, and the shunt LC resonators by using microstrip quarter-wavelength short-circuited stubs which require usually via-holes through the substrate. In this paper, we choose the topology in Fig. 5 because the series LC resonators can be easily realized by using microstrip quarter-wavelength open stubs.

The central frequencies of the dual-bands of the filter are 1.8 GHz and 2.4 GHz, respectively. The ripple in the passbands is chosen as 0.01 dB. The equal-ripple bandwidth of both the first and second passband is 2.78%, i.e., 50 MHz and 67 MHz, respectively.

By using the formulas given in Sect. 2, we calculated the values of all elements in Fig. 5. We have $J_{01} = J_{23} = 0.02335$, $J_{12} = 0.0286$, $J_a = J_b = 0.06$, $C_{x1} = C_{x2} = 1.2649$ pF, $L_{x1} = L_{x2} = 4.6355$ nH, $C_{a2} = C_{b2} = 1.3912$ pF, $L_{a2} = L_{b2} = 4.215$ nH. The frequency response of the dual-band BPF in Fig. 5 is plotted in Fig. 8(a). Figures 8(b) and (c) provide close-up views of the dual passbands at about 1.8 GHz and 2.4 GHz, respectively. It is seen that both the center frequencies and bandwidths of the dual passbands meet the design specifications.

Figures 9(a) and (b) show a quarter-wavelength microstrip open stub and its equivalent series L_aC_a resonator, respectively. The microstrip open stub has a length l_a, a width w_a, a characteristic impedance Z_a, and is quarter-wavelength at ω_a. So we have

$$l_a = \frac{\pi c}{2\omega_a\sqrt{\varepsilon_{eff}}},\ \omega_a = \frac{1}{\sqrt{L_aC_a}} \tag{37}$$

where c is the speed of light in free space, ε_{eff} is the effective dielectric constant of the stub. Let the reactance slope parameter of the input reactance of the open stub and that of the LC resonator equals to each other at ω_a, we get [15]

$$Z_a = \frac{4\omega_a L_a}{\pi} = \frac{4}{\pi\omega_a C_a} \tag{38}$$

From (37) and (38), the lengths and widths of the quarter-wavelength lines and open stubs can be determined readily.

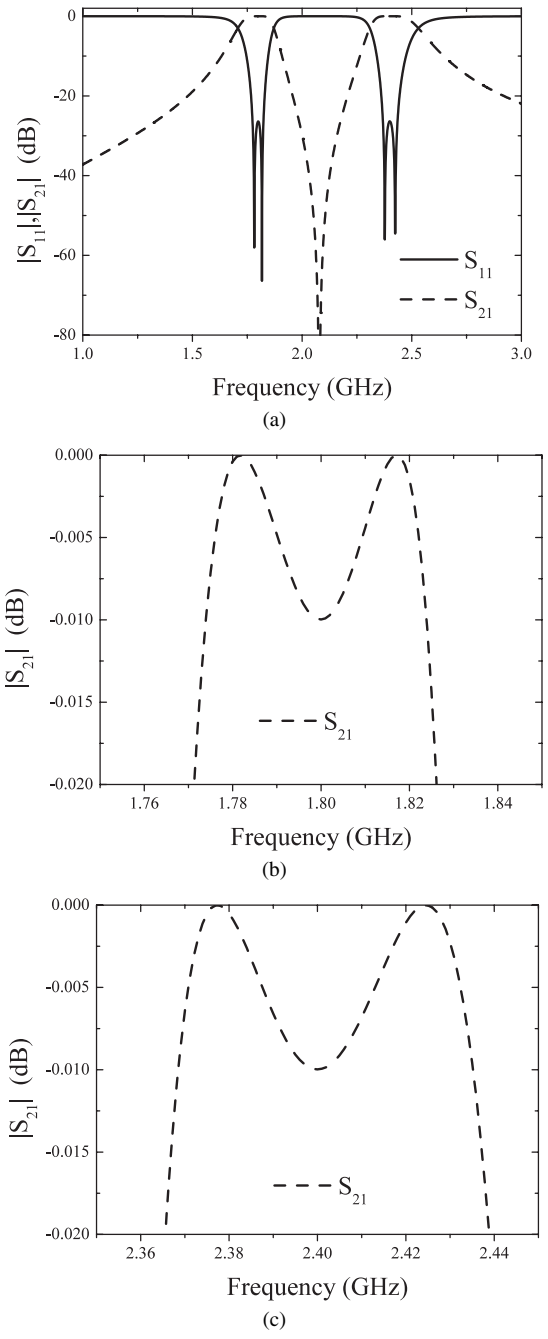

Fig. 8 (a) Circuit simulated response of a dual-band BPF with central frequencies of 1.8 GHz and 2.4 GHz, respectively, (b) a close-up of the passband at frequencies around 1.8 GHz, and (c) a close-up of the passband at frequencies around 2.4 GHz.

Figure 10 shows the configuration and dimensions of our designed dual-band filter. The four series resonators in Fig. 5 are implemented by four open stubs with lengths l_2, l_4, l_6, and l_8, respectively. The five J-inverters are realized by five pieces of quarter-wavelength transmission lines with lengths l_1, l_3, l_5, l_7, and l_9, respectively.

A commercial substrate Duriod 6010 with a relative dielectric constant of 10.2, a loss tangent of 0.0023, and a thickness of 0.635 mm is used in the design. By using a

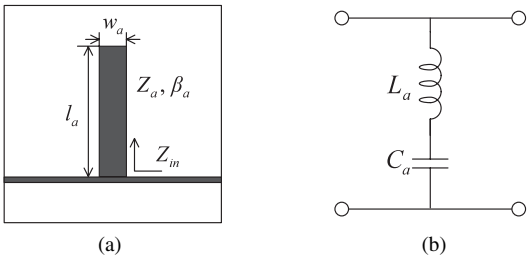

Fig. 9 (a) A quarter-wavelength microstrip open stub, and (b) its equivalent series *LC* resonator.

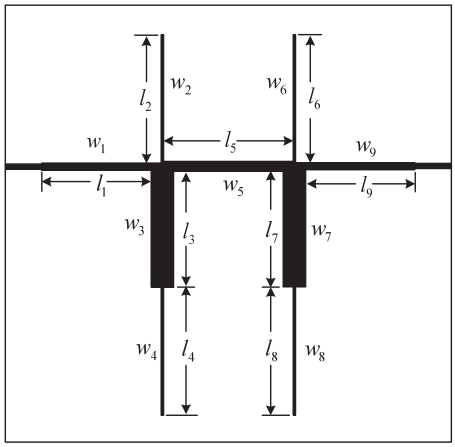

Fig. 10 Microstrip realization of dual-band bandpass filter.

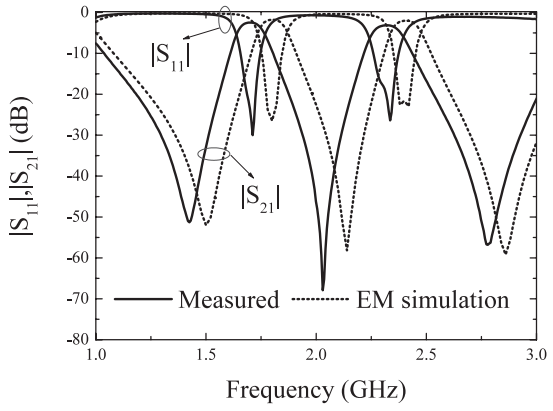

Fig. 11 Simulated and measured responses of the fabricated dual-band BPF with central frequencies of 1.8 GHz and 2.4 GHz.

full-wave electromagnetic solver, Sonnet em [16] and expressions (37) and (38), we get $l_1 = l_9 = 13.5$ mm, $w_1 = w_9 = 0.8$ mm, $l_2 = l_6 = 13.55$ mm, $w_2 = w_6 = 0.3$ mm, $l_3 = l_7 = 12.4$ mm, $w_3 = w_7 = 2.4$ mm, $l_4 = l_8 = 13.7$ mm, $w_4 = w_8 = 0.2$ mm, $l_5 = 12.6$ mm, and $w_5 = 1.0$ mm. The characteristic impedances of the lines are: $Z_1 = Z_9 = 42.4\,\Omega$, $Z_2 = Z_6 = 65.3\,\Omega$, $Z_3 = Z_7 = 21.3\,\Omega$, $Z_4 = Z_8 = 74.8\,\Omega$, and $Z_5 = 37.6\,\Omega$.

Figure 11 provides a comparison of the simulated and measured characteristics of the filter. The solid lines are measured response of the fabricated filter, using a network analyzer HP8722ES. The dash lines are simulated curves of the microstrip filter shown in Fig. 10, using Sonnet em. Both the dielectric and conductor (with a conductivity of $s = 5.8 \times 10^7$ S/m of copper) loss are taken into account in the simulation. The agreement over the dual bands is good except a frequency shift occurs between the simulated and measured responses. Such a frequency shift is observed in most previous reports of filters, and is mainly caused by the deviation of dielectric constant between the nominal and its real values, and by the fabrication tolerance of the filter. A transmission zero at about 2.1 GHz is clearly observed, which produces sharp and large attenuations between the dual passbands of the filter. By observing Fig. 4 or Fig. 5, we can see that this in-between transmission zero is produced by the series $L_{a2}C_{a2}$ resonator and series $L_{b2}C_{b2}$ resonator. From Eq. (11), we find that both $L_{a2}C_{a2}$ resonator and $L_{b2}C_{b2}$ resonator resonate at $\omega_0 = (\omega_1\omega_2)^{1/2}$. As a result, the shunt branches formed by $L_{a2}C_{a2}$ and $L_{b2}C_{b2}$ become short-circuited at frequency ω_0, and a transmission zero is thus produced at ω_0. Obviously this transmission zero is fixed at ω_0. These series resonator branches correspond to the quarter-wavelength open stubs with lengths l_2 and l_6 in the microstrip filter shown in Fig. 10. A further analysis reveals that the two-section open stub with lengths l_3 and l_4 (or l_7 and l_8) in Fig. 10 produces a pair of transmission zeros, one in the lower side, and the other in the upper side of the dual-band filter, as shown in Fig. 11. The positions of these transmission zeros can be moved by varying the ratio of the characteristics impedances of the two-section transmission lines.

4. Conclusion

A new synthesis method of dual-band microwave BPFs is described. By implementing two successive frequency transformations, a dual-band BPF is obtained from a prototype lowpass filter. New topologies of dual-band BPFs are obtained, and their realizations are made easy by carrying out circuit conversions using admittance inverters. The overall size of the developed microstrip filter is small compared with previously reported dual-band filter using external dual-band impedance matching networks. The design example in a microstrip form provides a good agreement between the measured and simulated frequency response of the filter, and verifies thereby the proposed theory.

Acknowledgments

This work is supported in part by the National Natural Science Foundation of China (GP60271029), in part by the High-Tech Research Center Project from the Ministry of Education, Culture, Sports, Science, and Technology, Japan, and in part by the CASIO Science Promotion Foundation.

References

[1] Y.L. Kuo and K.L. Wong, "Printed double-T monopole antenna for

2.4/5.2 GHz dual-band WLAN operations," IEEE Trans. Antennas Propag., vol.51, no.9, pp.2187–2192, Sept. 2003.
[2] H. Hashemi and A. Hajimiri, "Concurrent multi-band low-noise amplifiers theory, design and applications," IEEE Trans. Microw. Theory Tech., vol.50, no.1, pp.288–301, Jan. 2002.
[3] H. Miyake, S. Kitazawa, T. Ishizaki, T. Yamada, and Y. Nagatomi, "A miniaturized monolithic dual band filter using ceramic lamination technique for dual mode portable telephones," 1997 IEEE MTT-S Int. Microwave Symp. Dig., pp.789–792, 1997.
[4] L.C. Tsai and C.W. Hsue, "Dual-band bandpass filters using equal-length coupled serial-shunted lines and Z-transform technique," IEEE Trans. Microw. Theory Tech., vol.52, no.4, pp.1111–1117, April 2004.
[5] S.F. Chang, Y.H. Jeng, and J.L. Chen, "Dual-band step-impedance bandpass filter for multimode wireless LANs," Electron. Lett., vol.40, pp.38–39, Jan. 2004.
[6] J.T. Kuo and H.S. Cheng, "Design of cross coupled open-loop resonator bandpass filters with a dual-passband response," 2004 Asia-Pacific Microwave Conference Proceedings, pp.246–249, Dec. 2004.
[7] H. Uchida, H. Kamino, K. Totani, N. Yoneda, M. Miyazaki, Y. Konishi, S. Makino, J. Hirokawa, and M. Ando, "Dual-band-rejection filter for distortion reduction in RF transmitters," IEEE Trans. Microw. Theory Tech., vol.52, no.11, pp.2550–2556, Nov. 2004.
[8] X. Guan, Z. Ma, P. Cai, G. Li, Y. Kobayashi, T. Anada, and G. Hagiwara, "A dual-band bandpass filter synthesized by using frequency transformation and circuit conversion technique," 2005 Asia-Pacific Microwave Conference Proceedings, pp.2294–2297, Dec. 2005.
[9] G. Matthaei, L. Young, and E.M.T. Jones, Microwave Filter, Impedance-Matching Networks, and Coupling Structures, Artech House, Norwood, MA, 1980.
[10] K. Wada and O. Hashimoto, "Fundamentals of open-ended resonators and their application to microwave filters," IEICE Trans. Electron., vol.E83-C, no.11, pp.1763–1775, Nov. 2000.
[11] M.H. Hsu and J.F. Huang, "Annealing algorithm applied in optimum design of 2.4 GHz and 5.2 GHz dual-wideband microstrip line filters," IEICE Trans. Electron., vol.E88-C, no.1, pp.47–56, Jan. 2005.
[12] H.Y.A. Yim and K.K.M. Cheng, "Novel dual-band planar resonator and admittance inverter for filter design and applications," 2005 IEEE MTT-S Int. Microwave Symp. Dig., THP J-5, pp.2187–2190, 2005.
[13] H.M. Lee, C.M. Tsai, and C.C. Tsai, "Transmission-line filter design with fully controllable second passband," 2005 IEEE MTT-S Int. Microwave Symp. Dig., THP J-6, pp.2191–2194, 2005.
[14] C. Quendo, E. Rius, and C. Person, "An original topology of dual-band filter with transmission zeros," 2003 IEEE MTT-S Int. Microwave Symp. Dig., WE1D-7, pp.1093–1096, 2003.
[15] Z. Ma and Y. Kobayashi, "Design and realization of bandpass filters using composite resonators to obtain transmission zeros," 35th European Microwave Conference Proc., pp.1255–1258, Oct. 2005.
[16] Sonnet suite, ver. 9.52, Liverpool, Sonnet Software, NY, 2004.

Xuehui Guan was born in Jiangxi, China, in 1976. He received B.E. degree from Jiangxi Normal University, China, in 1998, and is currently pursuing his Dr. Eng. degree at Shanghai University. He is engaged in researches on microwave planar circuits.

Zhewang Ma was born in Anhui, China, on July 7, 1964. He received the B.Eng. and M.Eng. degrees from the University of Science and Technology of China (USTC), Hefei, China, in 1986 and 1989, respectively. In 1995, he was granted the Dr. Eng. degree from the University of Electro-Communications, Tokyo, Japan. He was a Research Assistant in 1996, in the Department of Electronic Engineering, the University of Electro-Communications, and became an Associate Professor there in 1997. Since 1998, he has been an Associate Professor in the Department of Electrical and Electronic Systems, Saitama University, Japan. From 1985 to 1989, he was engaged in research works on dielectric waveguides, resonators and leaky-wave antennas. From 1990 to 1997, he did studies on computational electromagnetics, analytical and numerical modeling of various microwave and millimeter wave transmission lines and circuits. His current research works are mainly on microwave and millimeter wave filters, measurements of dielectric materials and high temperature superconductors. He received Japanese Government (Ministry of Education, Culture, Sports, Science and Technology) Graduate Scholarship from 1991 to 1993. He was granted the URSI Young Scientist Award in 1993. From 1994 to 1996, he was a Research Fellow of the Japan Society for the Promotion of Science (JSPS). Dr. Ma is a member of IEEE. He has served on the Editorial Board of *IEEE Transactions on Microwave Theory and Techniques*, Review Board of *IEEE Microwave and Wireless Components Letters*, and Review Board of *IEICE Transactions on Electronics*, Japan. He is a member of the Steering Committee for 2002 and 2006 Asia Pacific Microwave Conference (APMC2002).

Peng Cai was born in Jiangxi, China, in 1980. He received B.E. degree from Hangzhou Dianzi University, Hangzhou, China, in 2001, and is currently pursuing his Dr. Eng. degree at Shanghai University. His current research works are mainly on microwave planar filters, microstrip antennas and computational electromagnetics.

Yoshio Kobayashi was born in Japan on July 4, 1939. He received the B.E., M.E., and D.Eng. Degrees in electrical engineering from Tokyo Metropolitan University, Tokyo, Japan, in 1963, 1965, and 1982, respectively. Since 1965, he has been with Saitama University, Saitama, Japan. He is now a professor at the same university. His current research interests are in dielectric resonators and filters, measurements of low-loss dielectric and high-temperature superconductive (HTS) materials, and HTS filters, in microwave and millimeter wave region. He served as the Chair of the Technical Group on Microwaves, IEICE, from 1993 to1994, as the Chair of the Technical Group of Microwave Simulators, IEICE, from 1995 to1997, as the Chair of Technical Committee on Millimeter-wave Communications and Sensing, IEE Japan, from 1993 to1995, as the Chair of Steering Committee, 1998 Asia Pacific Microwave Conference (APMC'98) held in Yokohama, as the Chair of the National Committee of APMC, IEICE from 1999 to 2000, and as the Chair of the IEEE MTT-S Tokyo Chapter from 1995 to1996. He also serves as a member of the National Committee of IEC TC49 since 1991, the Chair of the National Committee of IEC TC49 WG10 since 1999 and a member of the National Committee of IEC TC90 WG8 since 1997. Prof. Kobayashi received the Inoue Harushige Award on "Dielectric filters for mobile communication base stations" in 1995. He is a Fellow of IEEE and a member of IEE Japan.

Tetsuo Anada received the B.S. and M.S. degrees in Electrical Engineering from Kanagawa University in 1974, and Ph.D. degree from the University of Tokyo in 1991, respectively. From 1969 to 1970, he was with the Toshiba Corporation. In 1974, he joined the Department of Electrical Engineering at Kanagawa University as a research associate. In 1992 he became a lecture and an associate professor in 1994, a professor in 2000. In 1995, he was at University of Nottingham and Scheffield on leave from Kanagawa University. Since 1974, he has been engaged in research on microwave planar circuit and guided-wave optics.

Gen Hagiwara after graduated form Chiyoda Television Electronic Technical School in 1980, he joined Towa-Circuit Corp. and began works on the design of printed circuits. In 1987, he established the Link Circuit Inc., where he is currently engaged in the development of high-speed digital circuits and high-frequency analog circuits.